

# Experimental investigation on dynamic response of asphalt pavement using SmartRock sensor under vibrating compaction loading

Han-Cheng Dan<sup>a</sup>, Dong Yang<sup>a</sup>, Xiang Liu<sup>b,\*</sup>, An-Ping Peng<sup>a</sup>, Zhi Zhang<sup>a</sup>

<sup>a</sup> School of Civil Engineering, Central South University, Changsha, Hunan 410075, China

<sup>b</sup> School of Traffic & Transportation Engineering, Central South University, Changsha, Hunan 410075, China

## HIGHLIGHTS

- Dynamic response of pavement and vibrating drum were monitored by SR and HCF sensors.
- High frequency signals were used to analyze the dynamic response in vibrating compaction.
- Linear relation was established between acceleration of vibrating drum and compactness.
- Understanding of compaction mechanism in terms of acceleration and stress for particles.

## ARTICLE INFO

### Article history:

Received 25 November 2019

Received in revised form 6 February 2020

Accepted 25 February 2020

### Keywords:

Asphalt mixture  
Vibrating compaction  
SmartRock sensor  
Gyratory compaction  
Dynamic response

## ABSTRACT

Although compaction is one of the most critical steps during the construction of asphalt pavements, effective real-time technologies to detect the compactness of the asphalt mixture non-destructively are still rare. Currently, most methodologies in practice are experience-based, and few studies have provided insight into the particle interaction characteristics and quantitative response during the vibration compaction of asphalt pavements. Accordingly, both field and laboratory tests are conducted in this study to investigate the response of an asphalt mixture quantitatively under a vibrating compaction load at the meso-scale. First, a field test program is designed, and sensors (e.g., SmartRock and acceleration sensors) are used to measure the dynamic response of an asphalt pavement and the vibrating drum during vibrating compaction. The quantitative analysis reveals that the first three rolling impacts exert a significant and dominant compact effect on the asphalt mixture. Subsequently, a linear relationship between the acceleration of the vibrating drum and the vertical stress in the asphalt pavement is demonstrated. Furthermore, the SmartRock sensor is also employed in the laboratory test to detect the internal dynamic response under gyratory compaction, and the relationship between the compaction degree and the vertical stress in the asphalt mixture is established. Finally, three assessment methods for asphalt mixture compactness are proposed as characterization of the compactness by the acceleration of a vibrating drum, intermediate variables such as the stress of the mixture under a gyratory compaction, or acceleration and stress of the pavement. Comparison of the results illustrates that the dynamic response inside the mixture during the compaction can directly reflect the compaction degree of the asphalt mixture, and the compaction degree and the peak acceleration of the vibrating drum exhibit a strong linear correlation during the vibration rolling process.

© 2020 Elsevier Ltd. All rights reserved.

## 1. Introduction

With the rapid rise in highway traffic, more attention is being paid to road safety and comfort. Pavement quality directly affects the service life of the highway, and is also an important factor in

driving safety and comfort [1,2]. In general, the quality of a pavement decays gradually after it is opened to traffic, which causes the performance of the highway to decline and pavement diseases to occur [3,4]. It is known that climatic conditions, construction materials, construction quality, traffic volume, and particularly compaction quality, affect the performance of an asphalt pavement [5–7]. Therefore, an important measure to improve the service life of an asphalt pavement is to ensure its compaction effect during the construction process [8]. Currently, most asphalt pavements

\* Corresponding author.

E-mail addresses: [danhancheng@csu.edu.cn](mailto:danhancheng@csu.edu.cn) (H.-C. Dan), [bruceyoung@csu.edu.cn](mailto:bruceyoung@csu.edu.cn) (D. Yang), [xiangliu06@gmail.com](mailto:xiangliu06@gmail.com) (X. Liu), [zz768956@csu.edu.cn](mailto:zz768956@csu.edu.cn) (Z. Zhang).

are compacted by vibratory rollers. Under the action of the wheel weight and the exciting force of the vibrating roller, the aggregates in the asphalt mixture are rearranged to form a solid skeleton, and the rigidity as well as the modulus of the pavement accordingly increase [9]. Because of the complexity of the asphalt mixture properties and the lack of the fundamental understanding of compaction mechanisms, field compaction control is mostly experience-based in practice, which causes numerous problems such as under/over-compaction. Insufficient compaction of asphalt pavements is prone to cause rutting, water damage, cracking, and other pavement diseases [10–12]. Concurrently, excessive compaction will lead to flushing oil and aggregate crushing of the asphalt pavement [13]. Consequently, the quality of pavement compaction needs to be identified and controlled during the compaction process [14].

Compactness is an important index to characterize the degree of compaction and for the quality control of asphalt pavements. The traditional pavement compactness test typically adopts an empirical method to measure the density of the core drilling specimen of the asphalt pavement. It then compares the sampled density with the theoretical density in the laboratory, to determine the compaction degree of the pavement [7,15]. However, this method is expensive and destroys the integrity of the pavement. Furthermore, after the core drilling is filled, the pavement will possess a defective area, finally leading to pavement diseases under the coupling effect of the environment and vehicle loading [16,17]. While some non-destructive technologies (such as nuclear or non-nuclear density meters) have been presented to inspect pavement compactness [18], these methods are still inefficient to evaluate the compaction degree of a pavement from a point to an area [16].

Compared with the traditional method to study the compaction of asphalt pavements, some new technical approaches have been developed, such as numerical and advanced empirical methods [19,20]. For instance, Huang et al. [21] used the ABAQUS finite element software to simulate the pavement vibration compaction process and analyzed the influence of the excitation force and rolling speed of the roller. It was found that the compaction effect was better when the roller compactor adopted a strong vibration and low speed. Chen et al. [22] used discrete element method (DEM) to simulate the laboratory asphalt compaction and studied the porosity change of an asphalt mixture under vibration compaction. Its results were in good agreement with the laboratory compaction test results. Nevertheless, the existing numerical simulation method of asphalt compaction is mostly limited to laboratory tests, and cannot simulate an actual pavement compaction owing to the complex processes [23]. For instance, the numerical method establishes a complex numerical model with a low calculation efficiency and calculation accuracy. Moreover, the mechanical parameters of an asphalt mixture and the material temperature tend to change as rolling progresses. Therefore, it is difficult to use numerical software to study pavement compactness accurately during a field rolling process.

To overcome these difficulties, an intelligent compaction (IC) method was presented in recent decades [24]. IC is a non-destructive testing method for the real-time determination of pavement compaction based on the change in the acceleration response of the roller [25,26] with a series of IC measure values (ICMV) that characterize the compactness of the asphalt mixture [27]. Hu et al. [28] found that there was a good linear relationship between the ICMVs and asphalt pavement compactness. Correia et al. [29] demonstrated that the linear correlation between the calculated and measured compaction degrees by dynamic modulus ( $E_{\text{vib}}$ ) could reach 0.9 or more. However, Petersen [30] indicated that the correlation between the ICMVs and the field-measured data was poor. Rinehart et al. [31] and Mooney et al. [32] studied the harmonic component values (CMV (Compaction Meter Value),

CCV (Compaction Control Value), and THD (Total Harmonic Distortion)) during compaction. It was found that the correlation between the compaction effect characterized by these component values and the field test results was affected by multiple factors (e.g., the asphalt mixture type, subbase, environment temperature, and roller parameters). Therefore, there may be a large dispersion and deviation when the compactness is expressed by the ICMVs, and the relationship between the vibration signal of a vibrating wheel and the compactness of the corresponding asphalt mixture cannot be accurately established.

In summary, the existing research (regardless of the use of numerical or empirical methods) does not specifically study the relationship between the internal vibration trend of a pavement and the responses of the associated roller during the compaction process. Thus, this leads to uncertainty in the evaluation of the compaction degree of the asphalt pavement. This is primarily because no suitable approaches can be utilized to investigate the internal dynamic response in an asphalt pavement in real time. In this study, field and laboratory tests were planned with a real-time particle sensor (i.e., SmartRock sensor) embedded in an asphalt mixture, to investigate the internal dynamic response of the corresponding pavement during vibrating compaction. These were expected to establish the relationship between the dynamic responses of the pavement, vibrating roller, and material to evaluate the compaction degree of the asphalt pavement.

## 2. Field test of dynamic response of asphalt pavement

### 2.1. SmartRock

SmartRock is a sensor that was developed and embedded in granular materials to monitor stress, deformation, and stability [33–35]. It was originally used in railway engineering to detect the stability of railway ballast [36]. The SmartRock sensor has a strong high-temperature resistance, so that it can be used in the high-temperature paving and compaction of an asphalt pavement construction [37]. An acceleration transducer, strain gauge, temperature sensor, gyroscope, and Bluetooth module are integrated in the SmartRock particle (SRP). Therefore, the data can be wirelessly collected in real-time in relation to the stress, vibration acceleration, and angle of rotation in the studied asphalt pavement under an external load. Further, its sampling frequency is 100 Hz. The maximum size of the SmartRock sensor was customized to be approximately 25 mm, which was close to the maximum grain size of the coarse aggregate in asphalt mixtures. Further, its outermost shell had an improved adhesion to the asphalt (Fig. 1).

In addition, it should be pointed out that the signal of acceleration is collected by the acceleration transducer in the SmartRock sensor, and the signal of stress is collected by the strain gauge with taking the temperature into account by the following equation.

$$\sigma = \frac{(U - U_0 - b \ln T - c) \times 10}{aA \times 10^6} \quad (1)$$

where  $U$  is the voltage signal recorded by the SmartRock sensor;  $U_0$  is the basic voltage signal before compaction;  $T$  is the temperature recorded by SmartRock sensor;  $A$  is the area of the strain gauge, and  $a, b, c$  are calculation coefficients. The SmartRock is a high precision sensor, and its acceleration, voltage, and angle data accuracy can reach 0.01 g, 0.01 V, and 0.01°, respectively.

### 2.2. Experiment program

The pavement vibration rolling field test was performed on a lower course of an asphalt concrete pavement, with a thickness of 80 mm, in the Chongshui Expressway in Guangxi Province,

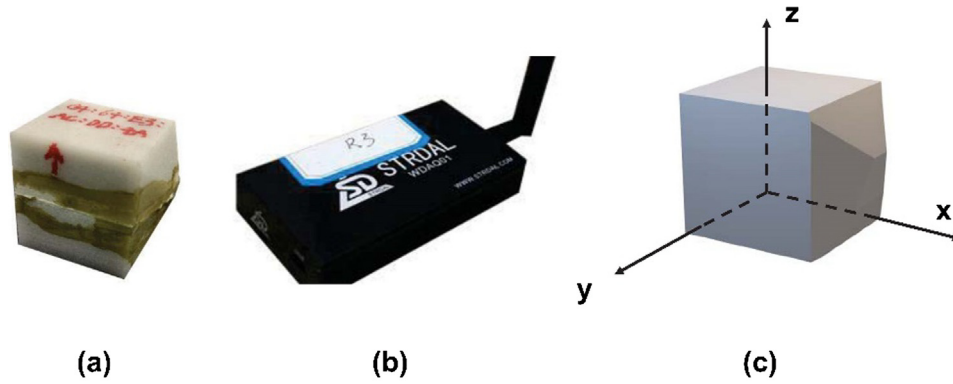


Fig.1. Data acquisition system: (a) SmartRock sensor, (b) Signal collector, (c) Coordinate system.

China. The compacted material was AC-25, whose gradation is presented in Fig. 2. The technical information of bituminous binder is listed in Table 1. The vibratory roller was BW203 AD-4 with double drums, and its actual working parameters are listed in Table 2.

The SmartRock sensor was embedded in the lower course of the pavement, approximately 20–30 mm to the top surface. For the data collection and sorting, the SmartRock sensor was so placed that its vertical direction (z), rolling direction (y), and lateral direction (x) coincided with the z-, y-, and x-axis, respectively, of the coordinate system of the sensor. The SmartRock data were collected by a WDQ1 (Wireless Data Acquisition 1) signal data receiver (Fig. 1(b)). During the compaction process, the acceleration signal of the vibrating drum was collected by an acceleration sensor named HCF, which was fixed on the vibration shaft of the rolling drum, and received by the supporting USB gateway. The data accuracy of the HCF can also reach 0.01 g. In the rolling direction, the data record area was selected approximately 25 m before and after the measuring point. After each rolling, a non-nuclear density meter was employed to detect the compactness of the compacted mixture near the measuring point. It need to be pointed

out that the parameters setting of roller cannot be considered because the frequency and amplitude of vibration rolling is determined according to the construction specification. Therefore, the roller setting is kept constant during compaction process to ensure the compaction quality. In addition, to ensure the accuracy of the test, the roller moved at a constant speed when passed the observation point to eliminate the fluctuation of signal for start and deceleration. The schematics of the field test, sensor installation, and rolling site are shown in Figs. 3 and 4.

In the process of asphalt pavement paving, the asphalt mixture was compacted by vibration roller (vibration rolling) for 8 times, and as a matter of fact, after the vibration compaction, the rubber rollers (static rolling) were employed to carry out subsequent compaction, which is not included in this paper and we just focused on the vibration rolling.

2.3. Data processing

Owing to the high sensitivity of the SmartRock sensor, multiple vibration signals are collected, such as the signals originating from

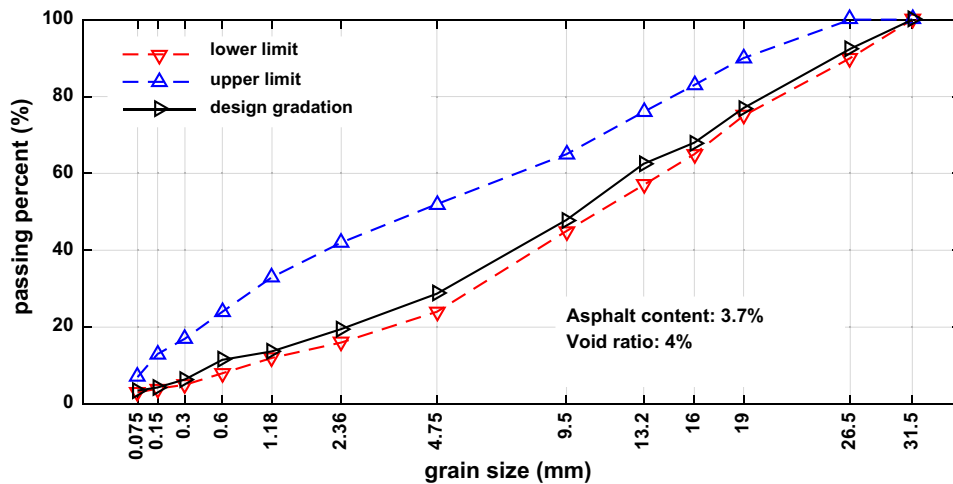


Fig. 2. Parameters of the material and grades.

Table 1  
Technical information of bituminous binder.

Parameter	Value	Requirement	Methods (JTG E20-2019) [38]
Penetration (25 °C, 100 g, 5 s)	63 (0.1 mm)	60–70 (0.1 mm)	T0604
Ductility (5 cm/min, 15 °C)	≥100 (cm)	≥100 (cm)	T0605
Softening Point	49 (°C)	≥47 (°C)	T0606
Dynamic Viscosity (60 °C)	≥200 (pa·s)	≥200 (pa·s)	T0620

**Table 2**  
Working parameters of BW203 AD-4.

Operating Weight	Static Weight at Front Drum	Drum dimension: Diameter/width	Frequency	Excited force	Driving speed
13000 kg	6500 kg	1240 mm × 2140 mm	50 Hz	84 kN	4.5 km/h

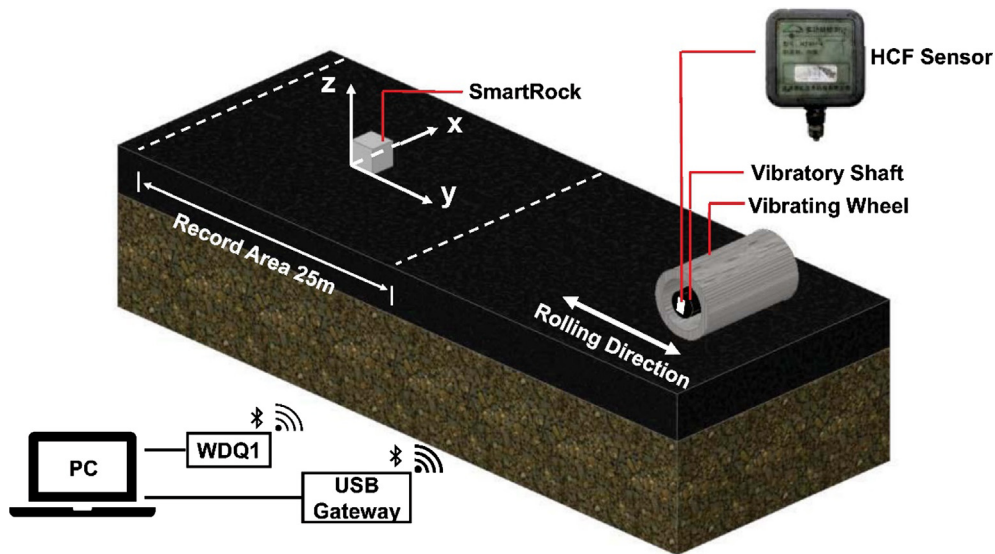


Fig. 3. Diagrams of the field test arrangement and the sensor layout.

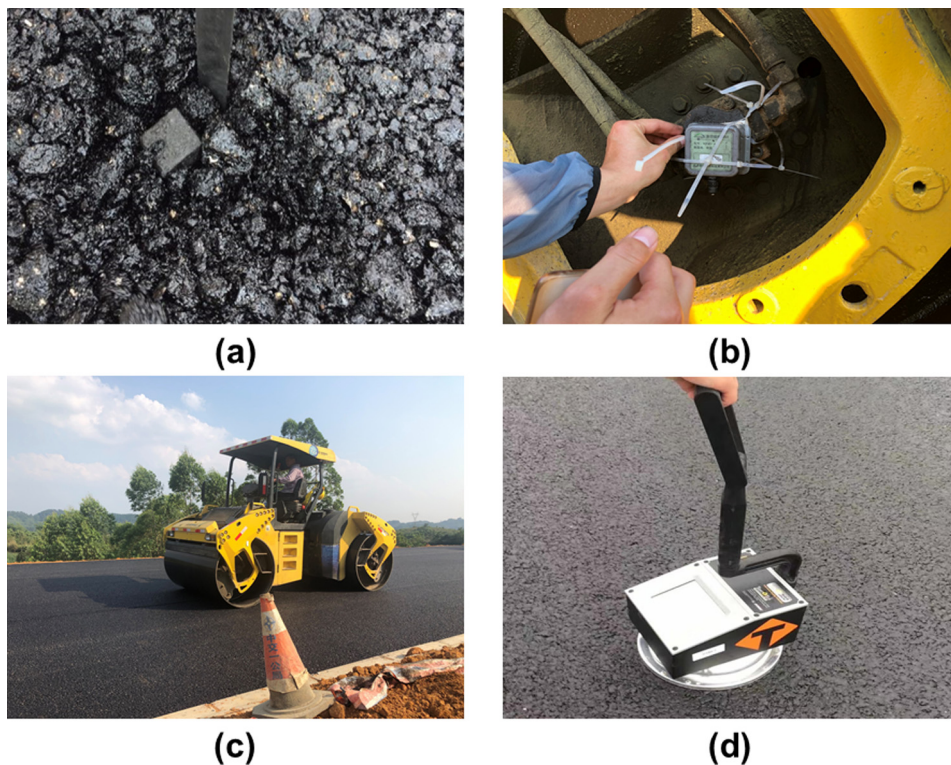


Fig. 4. Field test program: (a) Embedding of the SmartRock sensor in the asphalt mixture; (b) Installation of an acceleration sensor on the vibrating drum; (c) Pavement rolling; (d) Compaction degree test.

the pavers and other grouped rollers in the neighboring lanes. For vibratory rollers, the collision and friction of the shafts and bearings generate vibration signals with different frequencies. Signifi-

cantly, the attenuation of a high-frequency vibration is mixed with a low-frequency vibration, and it is impossible to be differentiated from the above low-frequency signals. Therefore, the signals

from the SmartRock and HCF were needed to be digitally filtered. The filtering conditions were set based on the working frequency of the vibration roller, and the collected data were filtered by the frequency domain method [39]. A band-pass filter code was written with MATLAB, and the measured data were filtered between 48 and 52 Hz, according to the working frequency of the roller, and the low-frequency signals were removed. Finally, the dynamic response data of the asphalt pavement under the vibration roller were obtained. An example band-pass filtering process is displayed in Fig. 5.

After the band-pass filtering of the measured vibration signal, the obtained vibration acceleration and stress time history curves of the paved layer are presented in Figs. A1–A4 in the Appendix section. Further, the Euler angle (rotation angle) is recorded and supplemented in Fig. A5. In this project, the embedded SmartRock sensor captured the temperature change inside the asphalt mixture in real time, which is displayed in Fig. 6. It can be seen that the temperature is not consistent with the actual temperature in engineering; this is because of the slow heat conduction process at the beginning when SmartRock was exactly embedded. Based on the research by Wang et al. [37], PaveCool, a computer tool developed by the Minnesota Department of Transportation [40], was applied to evaluate the temperature change during the compaction process for reference. It is pointed out that the initial temperature of the asphalt mixture was 137 °C measured by the infrared thermometer.

2.4. Dynamic response of asphalt pavement

Based on the figures in the Appendix, the peak value of the dynamic response was selected to reflect the intensity and is illustrated in the histograms of Figs. 7 and 8. It can be seen that both the acceleration and stress in the pavement decrease with the number of rollings; concurrently, those in the z direction dominate the dynamic response compared with those of in the x and y directions. When the roller travels directly above the SmartRock sensor, the acceleration and stress of SmartRock in the x, y, and z directions fluctuate significantly. For instance, the stresses in the x and y directions are 5% and 57% of those in the z direction, respectively. Therefore, the influence of the vibrating roller on the internal vibration acceleration and stress of the pavement is mainly concentrated in the z direction. This is because the vertical exciting force acts as the main compaction energy to the asphalt mixture of the pavement.

To demonstrate the change in the regulation of the dynamic response during the vibrating compaction, the scatter plots of the peaks of the acceleration and stress in the three directions and

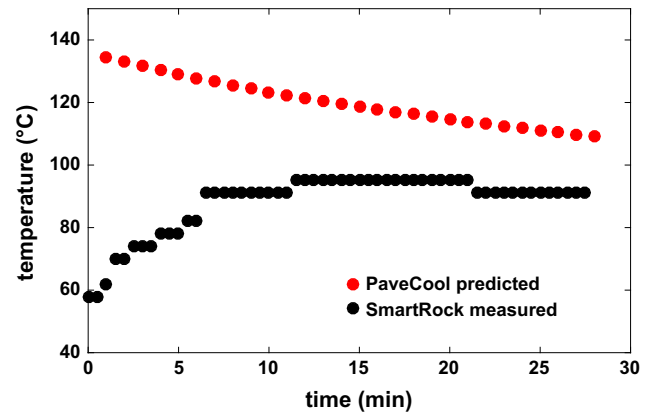


Fig. 6. Real-time temperature inside the asphalt mixture during the compaction process.

the rotation angle in the x direction are plotted and fitted by the power formula in Figs. 9 and 10. It can be seen that with the increase in the number of rollings, the peaks of the acceleration (0.49 g in the z direction and 0.41 g in the y direction) and stress (1.09 MPa in the z direction and 0.62 MPa in the y direction) in the vertical and rolling directions are gradually reduced. From the second pass, the stress in the vertical direction of each rolling is respectively 77%, 65%, 69%, 65%, 61%, 55%, and 59% of that in the first pass. Further, the stress in the rolling direction (y direction) is 73%, 56%, 27%, 24%, 27%, 21%, and 21% of that in the first pass, respectively. Apparently, the acceleration and stress changes between the former three rolling time are remarkable and gradually stabilized after the later compaction times, which exhibits a clear trend of the power function change. This is because the asphalt mixture gradually forms a stable skeleton structure during the former three rolling times. The strength and modulus of the mixture increase so that the internal dynamic response of the pavement under the vertical vibration load is reduced [41,42]. This phenomenon reflects that the former three rolling operations contribute the most to the compaction of the asphalt mixture. Furthermore, it can be noted from Fig. 9 that the vertical response (e.g.,  $a_z$  and  $s_z$ ) is more prominent than the horizontal response (e.g.,  $a_x$ ,  $a_y$ ,  $s_x$  and  $s_y$ ). For instance, the peak values of the acceleration and stress in the vertical direction are 0.49 g and 1.09 MPa, respectively, and the horizontal acceleration and stress in the y direction are 0.41 g and 0.62 MPa, respectively. Clearly, the degree of response is the most insignificant in the x direction. Fig. 9(b) displays that the stress of the particle decreases during the rolling

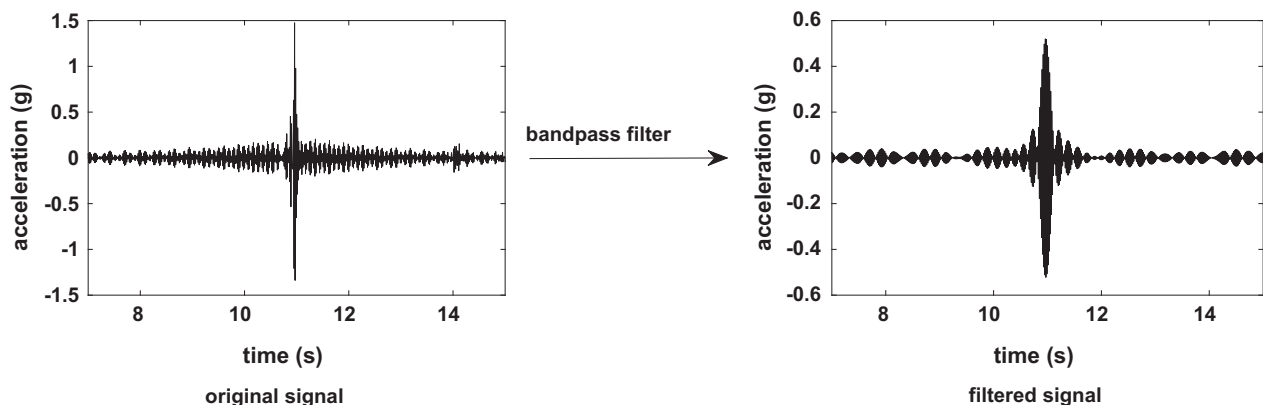


Fig.5. Band-pass filtering of the measured signal.

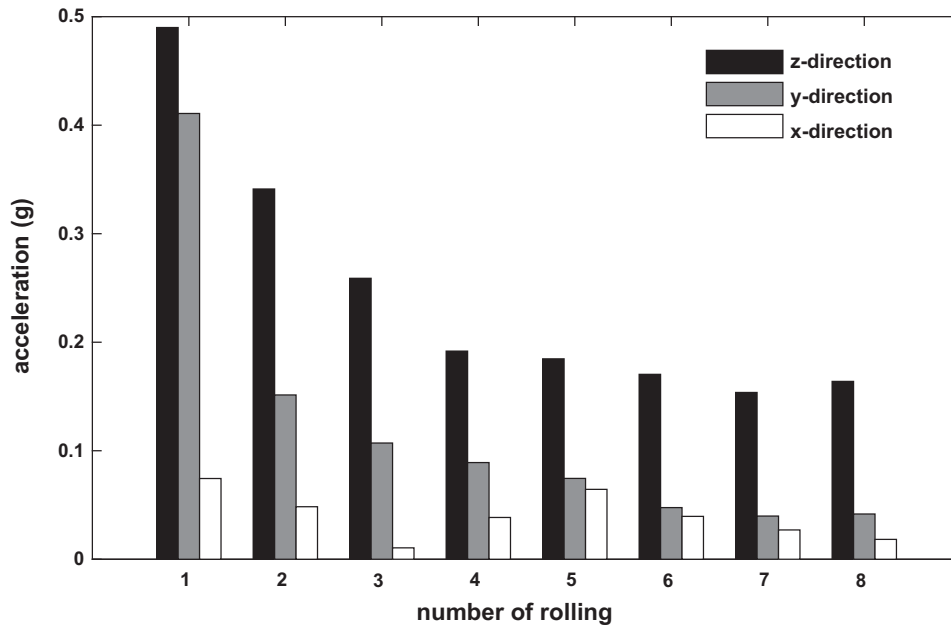


Fig. 7. Peak value of the measured acceleration in various directions in the pavement during the vibration rolling.

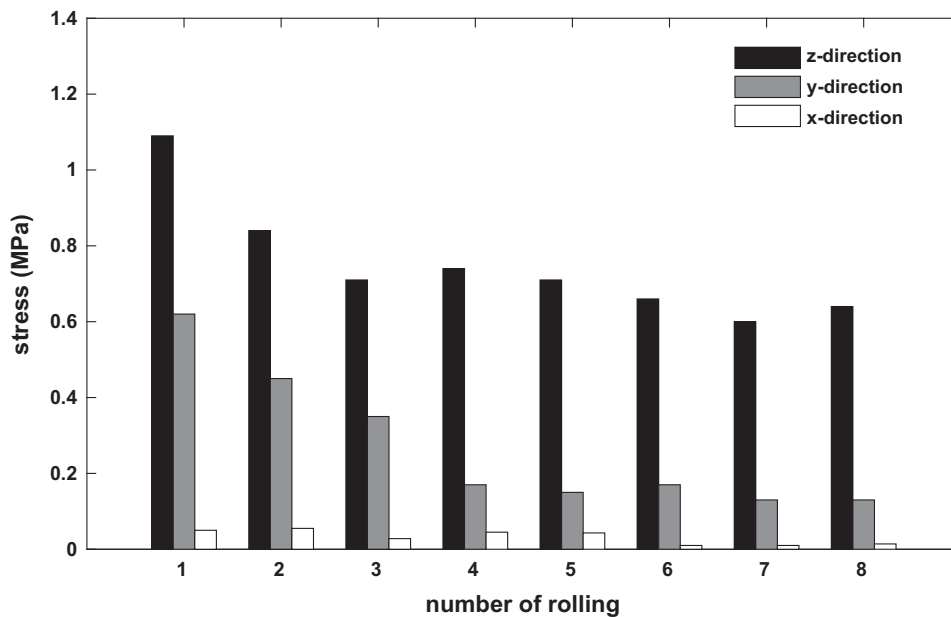


Fig. 8. Peak value of the measured stress in various directions in the pavement during the vibration rolling.

process, which is in contrast to the general understanding. It can be interpreted that under the initial condition, the compaction load is concentrated at the soft pavement owing to the low compactness and high temperature. Subsequently, the load is dispersed when the asphalt mixture becomes denser and the temperature drops.

To clarify the response difference for the three directional components (i.e., x, y, z), the rotation angle was utilized as a reference, which is shown in Fig. 10 and the Appendix. It should be noted that the rotation angle is much smaller than in the test results by Wang et al. [37]. First, for a comparison, we define an indicator as below.

$$\begin{cases} \Delta_A = \frac{A_1 - A_i}{A_1} \\ \Delta_\sigma = \frac{\sigma_1 - \sigma_i}{\sigma_1} \\ \Delta_\alpha = \frac{\alpha_1 - \alpha_i}{\alpha_1} \end{cases} \quad (2)$$

where  $A_1$ ,  $\sigma_1$ , and  $\alpha_1$  are the acceleration, stress, and rotation angle for the first rolling, respectively, and subscript  $i = 1, 2, 3, \dots, 8$  represents the rolling sequence.  $\Delta_A$ ,  $\Delta_\sigma$ , and  $\Delta_\alpha$  represent the relative deviations for the different responses (i.e., acceleration, stress, and rotation angle, respectively).

Based on Eq. (2), the calculated results are plotted in Fig. 11. It can be found that the acceleration and stress in the z direction (black line with solid circle) are always under those in the y direction (red line with solid diamond). This indicates that the aggregates rotate around the x coordinate and push each other so that they are subjected to the kneading of drum in the compaction process, with the aggregate rotation playing a relatively indistinctive role in the stress in the vertical direction. Apparently, the vertical vibrating force mainly forces the aggregates to be compressed downward and leads to a dominant vertical stress. The above

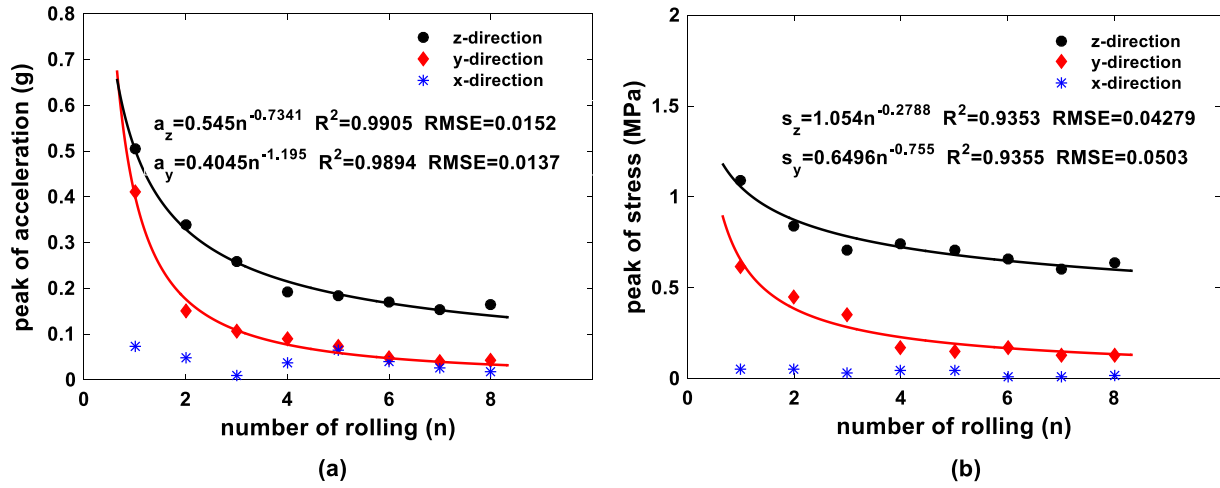


Fig. 9. Peak dynamic response of the pavement: (a) acceleration; (b) stress.

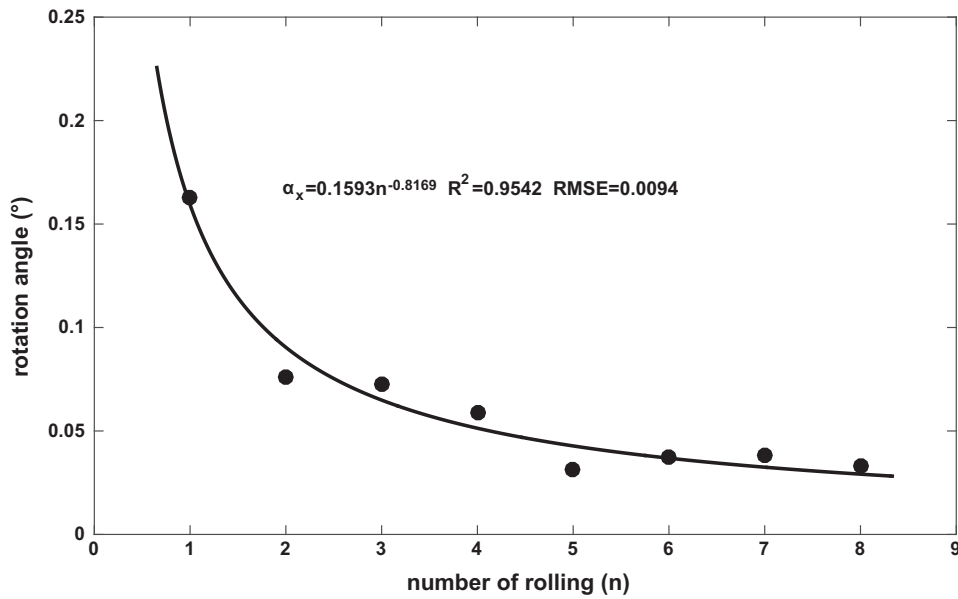


Fig. 10. Rotation angle of the SmartRock particle around the x-axis.

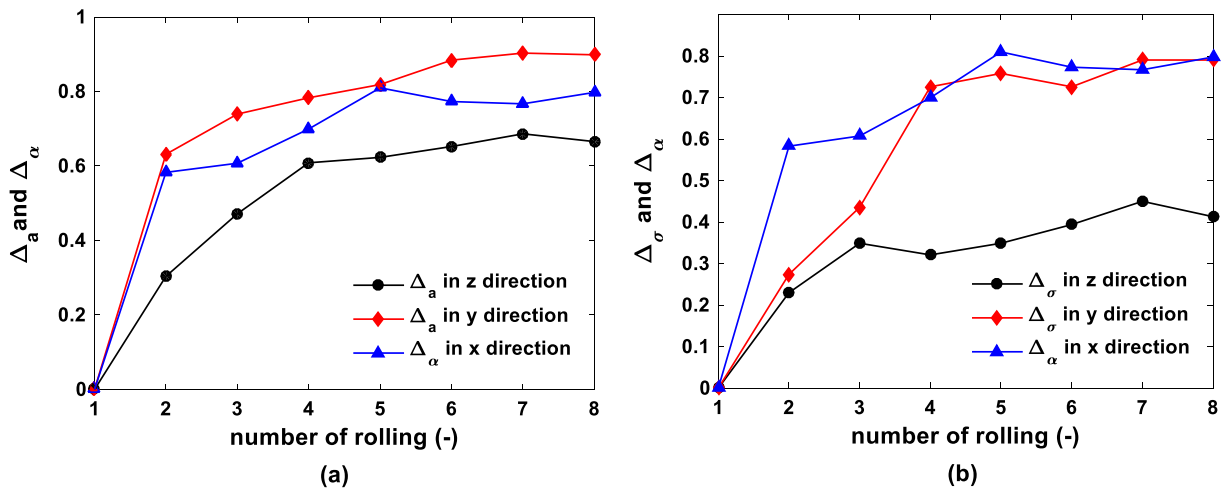


Fig. 11. Effect of the aggregate rotation on the dynamic response in terms of the acceleration and stress in different directions.

mechanism is also similar in terms of the acceleration of the aggregates.

Recalling Fig. 9, it should be noted that while the dynamic responses in the  $x$  direction are relatively scattered they also exhibit a tendency to gradually decrease when the mixture becomes denser. It can be inferred that during the compaction, the acceleration and stress in the  $x$  direction of the pavement are mainly generated by the lateral pressing between the aggregates that are subjected to a relatively slight kneading and compressing compared with those in the  $y$  direction.

In summary, the above discussion illustrates that the effects of the vertical vibration and compression dominate the contribution to the compaction. Further, the compaction in the horizontal direction mainly depends on the kneading and pushing between the drum of the roller and the aggregates of the mixture.

As mentioned above and according to the test results, the dominating dynamic response of the pavement under the excitation force in the vibration compaction process occurs in the vertical direction. Therefore, in this study, the response in the vertical direction of the pavement is selected for the analysis to establish the relationship between the pavement response and the vibrating drum of the roller.

For a vibratory roller, the area of contact of the vibrating drum with the pavement surface can be approximated as a rectangle according to the principle of area equivalence [43]. The formula for calculating the contact stress when the vibrating drum acts on a ground was proposed by Zhi et al. [44] as

$$p = \frac{13(G + F)}{DL} \quad (3)$$

For the BW 203 vibratory roller used in the field test, in this study, the maximum force of the vibrating drum on the ground is 149 kN, which is the sum of the drum weight ( $G$ ) and the exciting force ( $F$ ). Substituting the relevant parameters into Eq. (3), the maximum contact stress of the vibrating drum on the pavement is approximately 0.73 MPa. The internal vertical maximum stress of the asphalt mixture after being rolled by the vibratory roller eight times is reduced from 1.09 MPa to 0.64 MPa which is less than the contact stress. It can be obviously seen that the compaction of vibrating drum results in the change of stress state in the asphalt pavement. Therefore, it is logically to put forward the analysis on the dynamic response of a vibrating drum.

### 2.5. Dynamic response of vibration drum

During the vibratory rolling process, the pavement material is gradually compacted, and it will simultaneously induce a dynamical response by the vibratory roller. The vibrating acceleration signals of the vibrating drum before and after the measuring point selected by the HCF accelerometer are displayed in Fig. 12. Further, the average value of the peak value of the vibrating drum acceleration during each rolling time is taken as the effective peak of the acceleration during the rolling. When the vibrating drum passes the measuring point several times, the peak value of the vibration acceleration gradually increases. In general, the material damping is large when the asphalt mixture is under loose conditions, causing the mixture to undergo a considerable plastic deformation to absorb more compaction energy under the action of the roller [45]. As the compaction proceeds, the stiffness of the asphalt mixture increases, whereas the damping and the absorbed compaction energy decrease accordingly. Therefore, the acceleration of the roller increases gradually. The vibrating acceleration of the vibrating drum is presented in Fig. 13 to illustrate the variation law during the rolling.

It can be seen from Fig. 13 that the peak value of the vibrating drum acceleration changes significantly between the former three

times of rolling and then gradually stabilizes. Furthermore, it exhibits the same power function change as the vertical dynamic response of the pavement measured by the SmartRock sensor.

### 2.6. Variation in compaction degree during vibrating process

The compaction degree was tested by the non-nuclear density meter for eight rollings, and the results are shown in Fig. 14. It can be seen that the relationship between the compactness and the rolling number is a power function that is similar to that of the vibratory roller acceleration. To investigate the interdependency further, the relationship between the acceleration of the vibrating drum and the pavement compactness for each rolling time was fitted and is depicted in Fig. 15. This illustrates a good correspondence, which can be reflected by the variation in the compaction degree caused by the acceleration of the vibrating drum during the rolling process.

$$K = 0.3537A + 78.05 \left( R^2 = 0.9607 \text{ RMSE} = 0.4083 \right) \quad (4)$$

## 3. Laboratory gyratory compaction of asphalt mixture

In practical engineering, the SmartRock sensor cannot be widely applied to test the response of pavements, and an effective method is needed to establish the relationship between the compactness and the acceleration of the vibrating drum in directly. The field test revealed a strong relationship between the compactness of the mixture, internal response of the material, and response of the vibrating drum. To study the relationship between the internal dynamic response of the asphalt mixture and the material compactness further, the relationship between the compaction curve and the internal vertical stress curve during the compaction process of the mixture was investigated using the SmartRock sensor. For a good correspondence between the internal dynamic responses of the mixture obtained by the laboratory and field tests, it is necessary to select a reasonable laboratory molding method for the asphalt mixture. The Strategic Highway Research Program (SHRP) of the United States examined the performance correlation between an asphalt mixture specimen prepared by different molding methods and an on-site pavement core specimen. It was found that the performance of the asphalt mixture formed by the gyratory compaction method exhibited the highest correlation with the actual mixture performance of the pavement [46]. In addition to the axial pressure during the gyratory compaction, the rotation angle of the base caused the line connecting the center of the surface of a specimen and the bottom surface to form a cone during the rotation, thereby generating a horizontal shear force. The aggregates were rearranged under the action of the vertical pressure and horizontal shear force, forming a skeleton, which formed a compacted mixture structure. The above process can also simulate the rolling of a mixture by the rolling drum during an actual construction process. Therefore, in this study, the laboratory test employed the gyratory compaction method to investigate the relationship between the vertical internal stress and the compactness in the compaction process.

### 3.1. Material and experiment

The laboratory material was the same as that of the field test pavement. The gyratory compaction test selected the IPC global universal gyratory compactor. The rotation angle of the compactor during the operation was  $1.16^\circ$ . The rotational speed was 30 r/min, and the vertical pressure was set as 600 kPa. Before the compaction, the asphalt mixture was blended in an agitator at  $160^\circ\text{C}$ . After mixing and blending, half of the mixture was placed

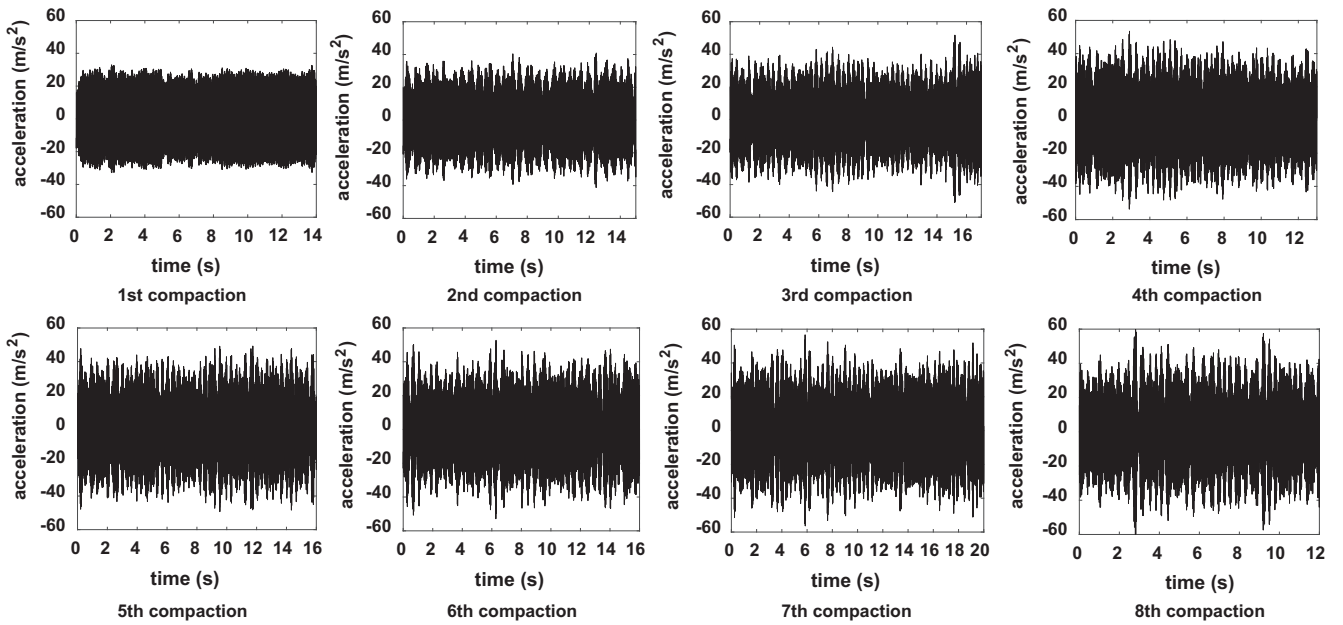


Fig. 12. Acceleration signal of the vibrating drum.

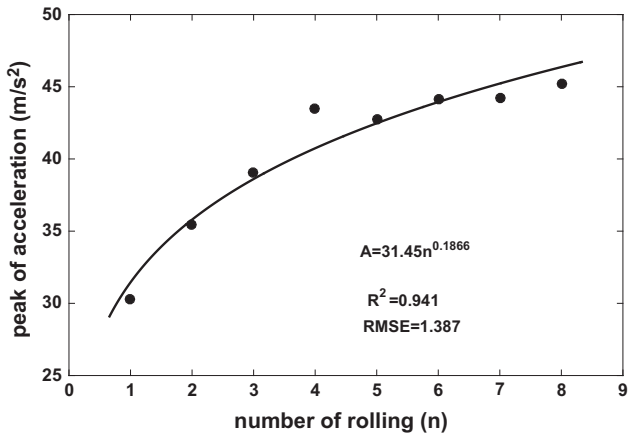


Fig. 13. Acceleration peak value of the vibrating drum during the compaction process.

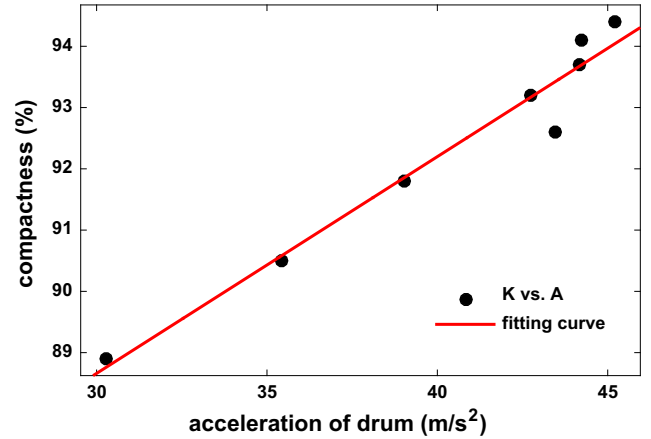


Fig. 15. Relationship between the acceleration of the vibrating drum and the pavement compactness during the rolling process.

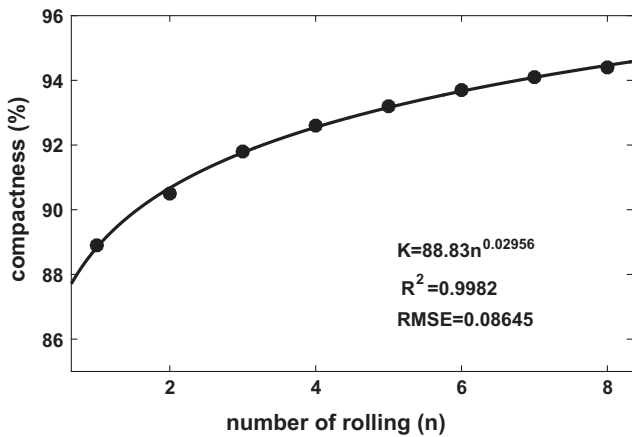


Fig. 14. Variation in the compactness for different rolling times.

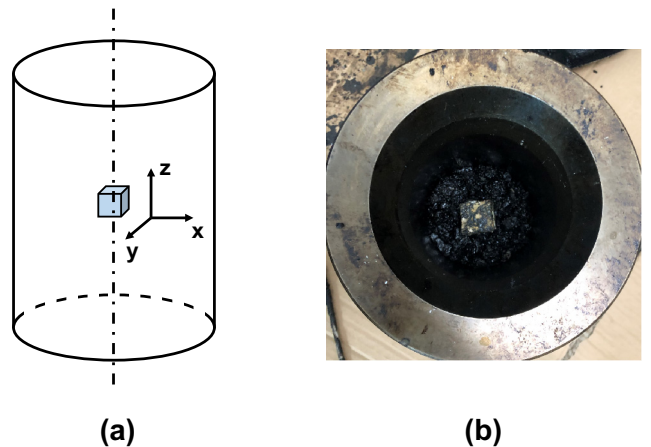


Fig. 16. Gyrotory compaction test: (a) SmartRock orientation; (b) SmartRock embedding.

into a mold, and a SmartRock sensor was placed in the center of the specimen. The vertical direction coincided with the z-axis of the sensor (Fig. 16(a)). Finally, the remaining mixture was filled into the mold to complete the embedding of SmartRock (Fig. 16(b)). The number of compaction circles was 120, and SmartRock collected 20 data per circle. Based on the rotation speed of the gyratory compactor, the data acquisition frequency was 10 Hz.

### 3.2. Compaction characteristics

In the compaction process, the vertical stress detected by SmartRock exhibits a periodic variation, as shown in Fig. 17, and the change period is the same as the rotation period of the gyratory compactor (2 s).

The mean value of the maximum and the minimum stress in the mixture during each cycle was defined as the internal mean stress of the mixture during the compaction process, indicating the overall stress variation of the mixture during the entire compaction process. The mean stress curve of the gyratory compaction is presented in Fig. 18 (black solid line). In the initial stage of the compaction, the axial stress inside the mixture is higher than the compaction stress of the compactor. This is because in this stage, SmartRock experiences a large displacement change instantaneously, and the collision between the particles is highly intense, resulting in the higher axial stress. As the number of compaction circles increases, the mean stress of the mixture first decreases and finally stabilizes, gradually approaching the compaction stress of the compactor. This trend is consistent with the conclusion drawn from the field vibration compaction test.

The height curve and the mean stress curve of the mixture obtained during the gyratory compaction are compared in Fig. 18 (red dash line), and it can be found that the mean stress exhibits the same variation characteristics as the height of the specimen. Therefore, the vertical stress of an asphalt mixture during compaction can be used as a reference for determining its compaction degree.

## 4. Evaluation of compaction degree

It can be seen from the field experiment and gyratory compaction that the higher the compaction degree of the asphalt mixture, the smaller the internal dynamic response (acceleration,

stress). For a better linear relationship between the vibration acceleration of the vibrating drum and the compaction degree of the mixture, the internal dynamic response of the mixture can potentially be used as an internal index. Furthermore, the acceleration of the vibrating drum can be employed as an external index, and the compaction degree of the asphalt mixture of the asphalt pavement can be characterized correspondingly.

### 4.1. Characterization of compaction degree based on accelerations of pavement and vibrating drum

The relationships between the internal acceleration of the pavement ( $a$ ), acceleration of the vibrating drum ( $A$ ), and compactness of the pavement ( $K$ ) are presented in Fig. 19. With the increase in  $A$  and  $K$ ,  $a$  decreases linearly, and their relationship can be obtained by linear regression as expressed in Eqs. (5) and (6).

$$a = -0.02192A + 1.134 \quad (R^2 = 0.9799 \text{ RMSE} = 0.01796) \quad (5)$$

$$K = -15.79a + 96.26 \quad (R^2 = 0.9428 \text{ RMSE} = 0.4928) \quad (6)$$

By combining Eqs. (5)–(7) is obtained and can be used to evaluate the compactness of the asphalt pavement based on the acceleration of the vibrating drum using the internal acceleration of the pavement during the vibrating compaction as an intermediate variable.

$$K = 0.3468A + 78.3 \quad (7)$$

### 4.2. Characterization of compaction degree based on pavement stress and acceleration of vibrating drum

The relations between the internal stress in the pavement ( $\sigma_f$ ), acceleration of the vibrating drum ( $A$ ), and compactness of the pavement ( $K$ ) are displayed in Fig. 20. With the increase in  $A$  and  $K$ ,  $\sigma_f$  decreases linearly, and their relationship can be obtained by linear regression, as expressed in Eqs. (8) and (9).

$$\sigma_f = -0.0276A + 1.868 \quad (R^2 = 0.878 \text{ RMSE} = 0.05873) \quad (8)$$

$$K = -11.57\sigma_f + 101.1 \quad (R^2 = 0.8912 \text{ RMSE} = 0.6796) \quad (9)$$

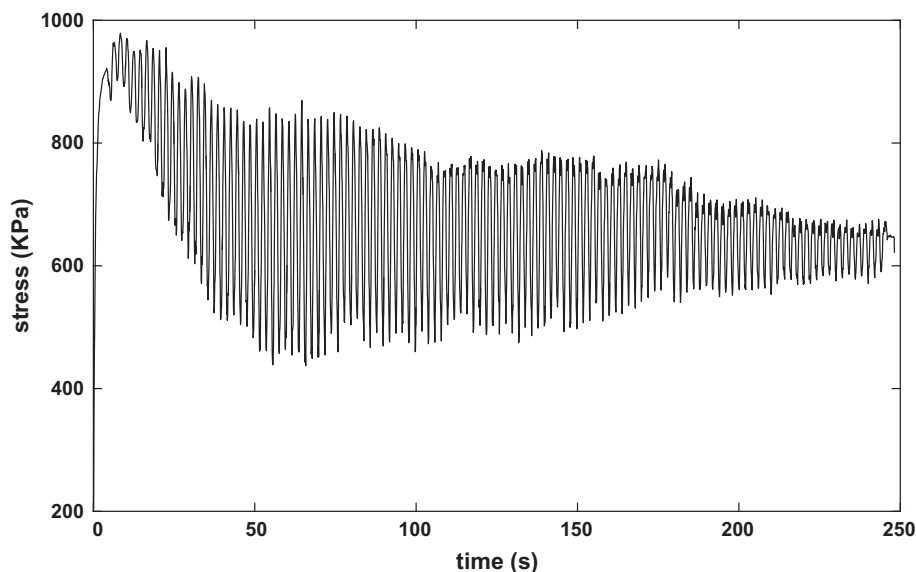


Fig. 17. Axial stress curve of the mixture during the gyratory compaction.

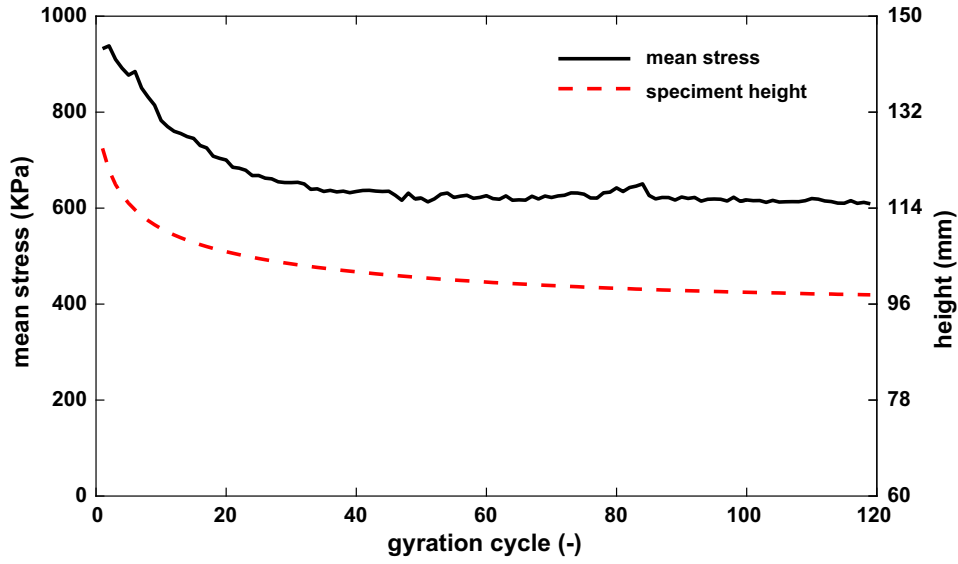


Fig. 18. Axial mean stress and height change curve during the gyratory compaction.

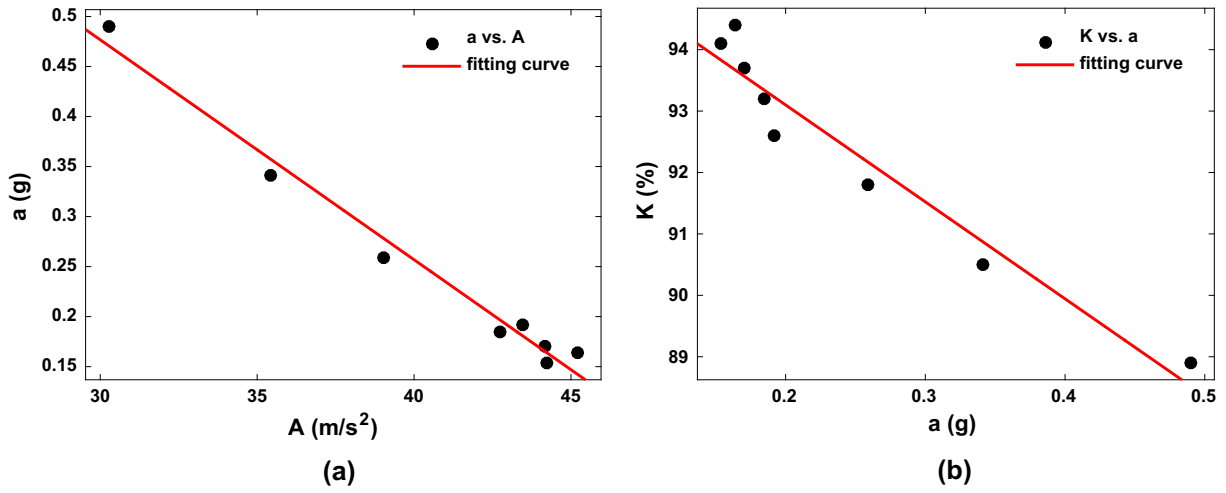


Fig. 19. Fitted relations between  $a$ ,  $A$ , and  $K$ : (a)  $a$  vs.  $A$ ; (b)  $a$  vs.  $K$ .

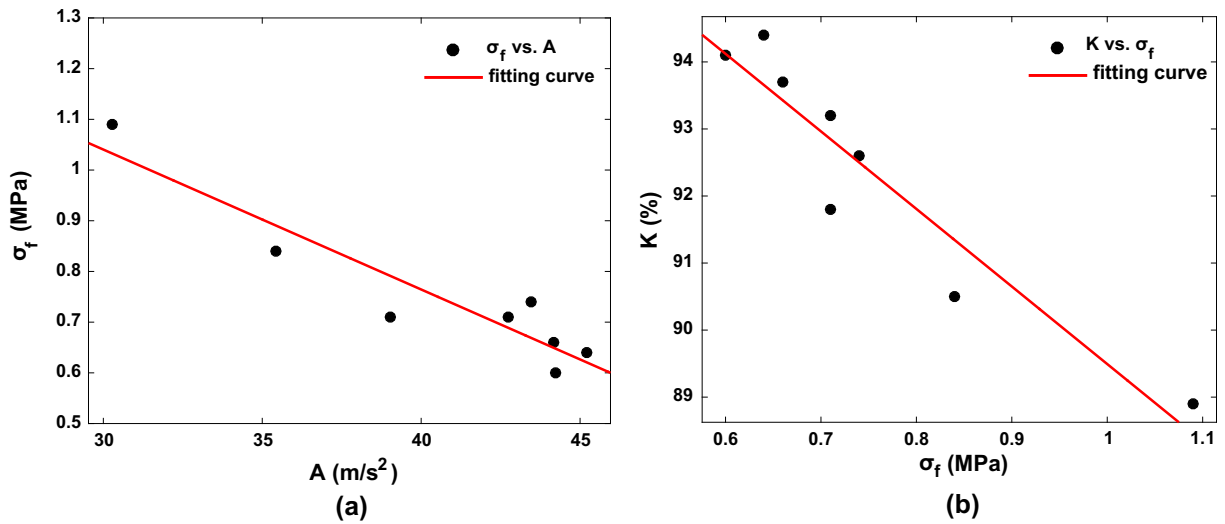


Fig. 20. Fitted relations between  $\sigma_f$ ,  $A$ , and  $K$ : (a)  $\sigma_f$  vs.  $A$ ; (b)  $\sigma_f$  vs.  $K$ .

Combining Eqs. (8)–(10), which can be used to evaluate the compactness of the asphalt pavement according to the acceleration of the vibrating drum using the internal stress of the pavement during the vibrating compaction, as an intermediate variable.

$$K = 0.3193A + 79.49 \quad (10)$$

4.3. Characterization of compaction degree based on stress of gyratory compaction and acceleration of vibrating drum

From the laboratory and field tests, it was revealed that the vertical stress inside the mixture gradually approached the compaction stress of the compaction equipment, and accordingly, the density of the mixture gradually reached its maximum value. The compactness and mean stress curves of the asphalt mixture in the gyratory compaction are shown in Fig. 21. In the initial stage of the compaction, the relative motion of the particles inside the mixture is relatively strong under the actions of the compaction stress and shearing force. Further, there is remarkable collision between the particles, resulting in a high internal stress in the mixture. As the compaction proceeds, the large particles in the mixture

gradually form a skeleton, and the stress curve is gradually stabilized at 0.6 MPa. This indicates that the compaction degree of the asphalt mixture is also basically stable. As presented in Fig. 21, the internal stress of the mixture is taken from the compactness curve in the gyratory compaction corresponding to the measured compaction degree in the on-site vibration rolling process. Furthermore, the relationship between the compactness, acceleration of the vibrating drum, and internal stress of the pavement can be obtained, and are shown in Fig. 22.

$$K = -43.81\sigma_g + 122 \left( R^2 = 0.9843 \text{ RMSE} = 0.2581 \right) \quad (11)$$

$$\sigma_g = -0.008086A + 1.004 \left( R^2 = 0.9789 \text{ RMSE} = 0.006784 \right) \quad (12)$$

By combining Eqs. (11)–(13) can be obtained to evaluate the compactness of the asphalt pavement according to the acceleration of the vibrating drum using the internal stress of pavement in the gyratory compaction as an intermediate variable.

$$K = 0.3542A + 77.87 \quad (13)$$

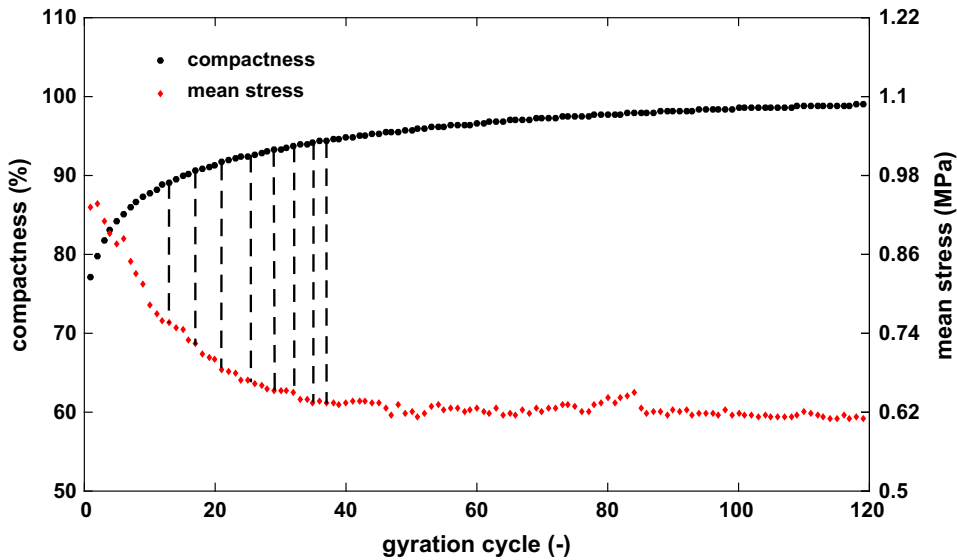


Fig. 21. Stress and compaction degree curve in the gyratory compaction.

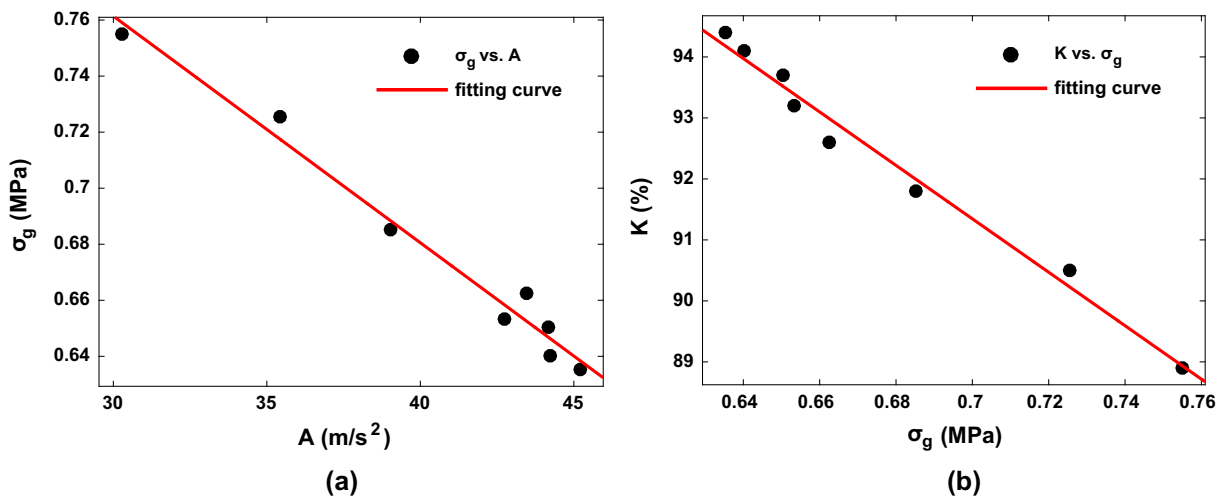


Fig. 22. Fitted relationship between  $\sigma_g$ ,  $A$ , and  $K$ , (a)  $\sigma_g$  vs.  $A$ ; (b)  $\sigma_g$  vs.  $K$ .

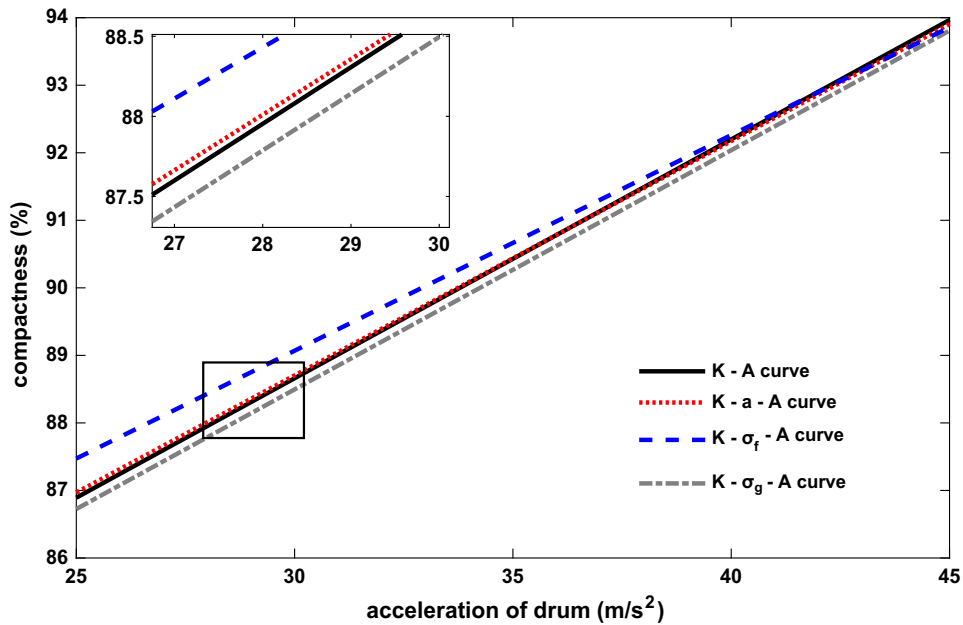


Fig. 23. Comparison between the different methods for evaluating the compaction degree.

#### 4.4. Comparison of different characterization methods

The above conversion methods (i.e.,  $K$ - $a$ - $A$ ,  $K$ - $\sigma_f$ - $A$ , and  $K$ - $\sigma_g$ - $A$ ) present expression similar to Eq. (3), and a comparison was performed to exhibit the differences (Fig. 23).

It can be seen from the comparison in Fig. 23 that the compaction degrees of the pavement which characterized by the three methods (i.e.,  $K$ - $a$ - $A$ ,  $K$ - $\sigma_f$ - $A$ , and  $K$ - $\sigma_g$ - $A$ ) and the formula of direct fitting by  $K$ - $A$  (Eq. (4)) are in good agreement. Therefore, this illustrates that the dynamic response inside the mixture during the compaction can directly reflect the compaction degree of the asphalt mixture. Further, the compaction degree and the peak acceleration of the vibration drum exhibit a strong linear correlation during the vibration rolling process.

#### 5. Concluding remarks

In this study, field and laboratory tests were conducted to investigate the response of an asphalt mixture under dynamic loading. For the field test, an experimental scheme was designed, and SmartRock and HCF sensors were used to monitor the dynamic response signal of an asphalt pavement as well as a vibrating drum under a vibration compaction. Furthermore, a SmartRock sensor was also employed in the laboratory test to detect the internal dynamic response in the gyratory compaction. Through a comprehensive analysis, the following conclusions can be drawn:

- (1) During the vibration compaction process, the internal dynamic responses (e.g., acceleration and stress of the aggregate) of the pavement are mainly concentrated in the vertical direction, which indicates that the action of the vertical vibration and compression dominates the contribution to the compaction, and the acceleration and stress in the asphalt mixture decreases as a power function.
- (2) The compaction in the horizontal direction mainly depends on the kneading and pushing between the drum of the roller and the aggregates of the mixture. Particularly, the acceleration and stress in the  $x$  direction of the pavement during the compaction are mainly generated by the lateral

pressing between the aggregates, which are subjected to a relatively slight kneading and compressing compared to those in the  $y$  direction.

- (3) A linear relationship is presented between the vibrating drum acceleration and the vertical stress inside the pavement.
- (4) In the gyratory compaction test of the asphalt mixture, it is found that there is a good linear correlation between the vertical stress and the compaction degree of the asphalt mixture.
- (5) The comparison of the four methods to evaluate compaction degree illustrate that the response in the mixture can not only reflect its compaction degree but also be used to establish the relationship between the compaction degree and the acceleration of vibrating drum. Consequently, the compaction degree and the peak acceleration of the vibration drum exhibit a strong linear correlation during the vibration rolling process.

Due to the practical experiment situation, only one on-site test was carried out, but another test was conducted in another project. Although the data is different due to the different test conditions (middle surface course, material and underlying conditions), the change law is similar. Furthermore, the location of the SmartRock may affect the signal data due to the energy dissipation in the process vibration rolling, and it will be studied in the future.

#### 6. Fundings

This research was supported by the National Natural Science Foundation of China (Grant No. 51308554 and 51778638), the Hunan Transportation Science and Technology Foundation of China (Grant No. 201622) and the Guizhou Transportation Science and Technology Foundation of China (Grant No. 2013-121-013 and 2019-122-006).

#### CRediT authorship contribution statement

**Dan Han-Cheng:** Conceptualization, Methodology, Writing - original draft, Funding acquisition. **Yang Dong:** Methodology, Data

curation, Investigation. **Liu Xiang:** Supervision, Writing - review & editing, Funding acquisition. **Peng An-Ping:** Project administration, Funding acquisition. **Zhang Zhi:** Investigation, Resources.

**Declaration of Competing Interest**

The authors declare that they have no known competing financial interests or personal relationships that could have appeared to influence the work reported in this paper.

**Appendix**

The filtered data for acceleration, stress and rotation angle are listed as below (Figs. A1–A5).

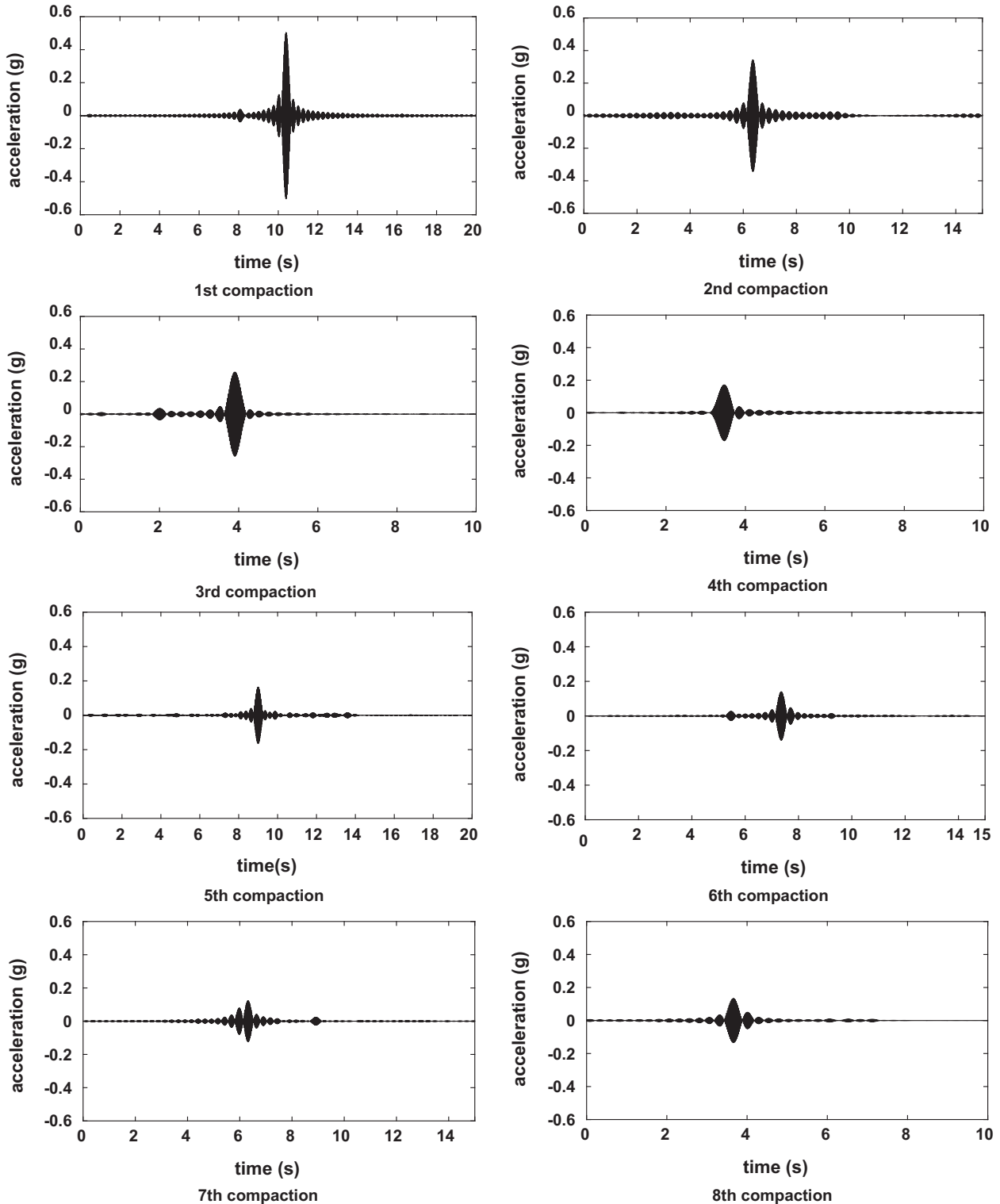


Fig. A1. measured acceleration of pavement in z-direction during vibration rolling.

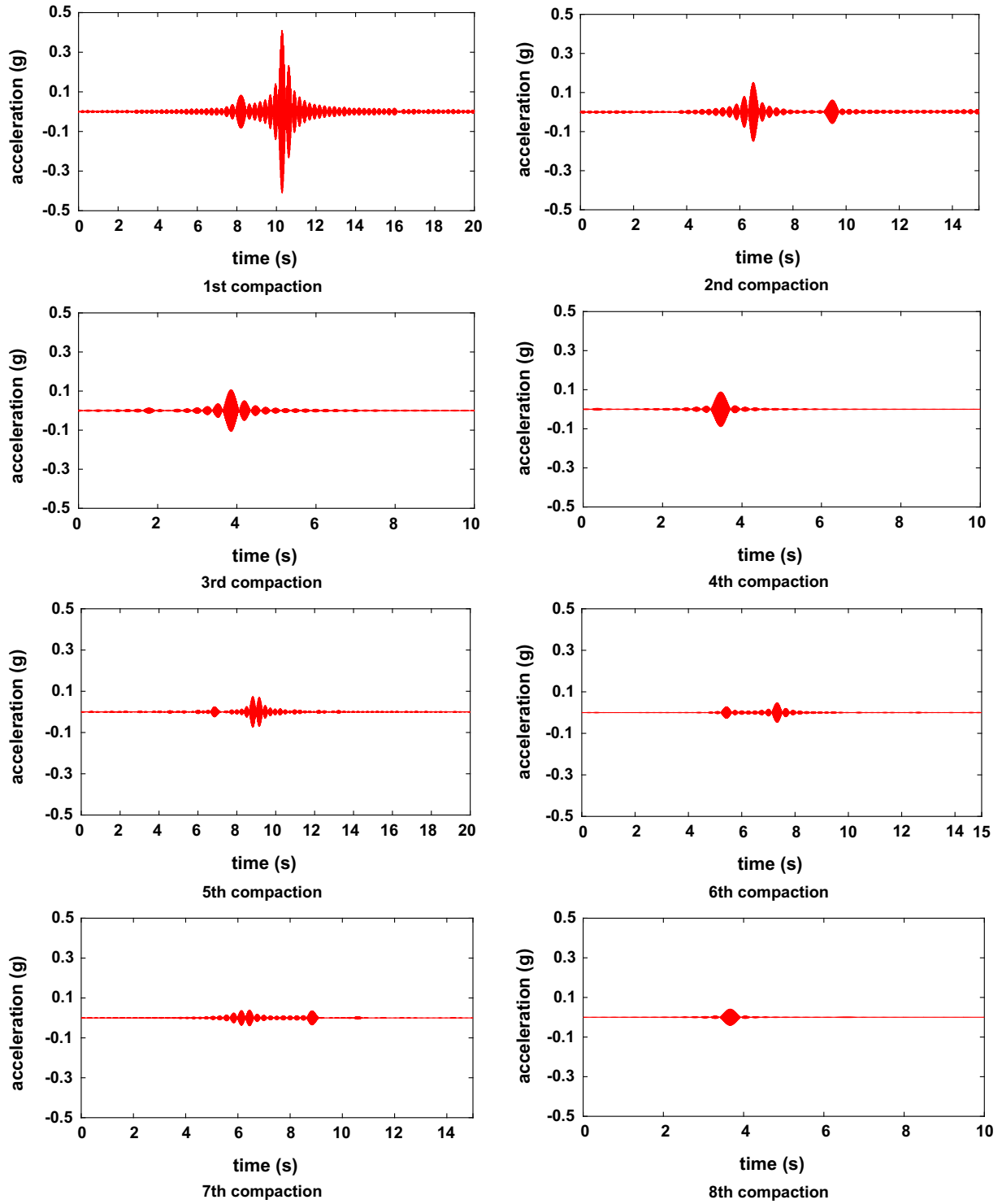


Fig. A2. measured acceleration of pavement in y-direction during vibration rolling.

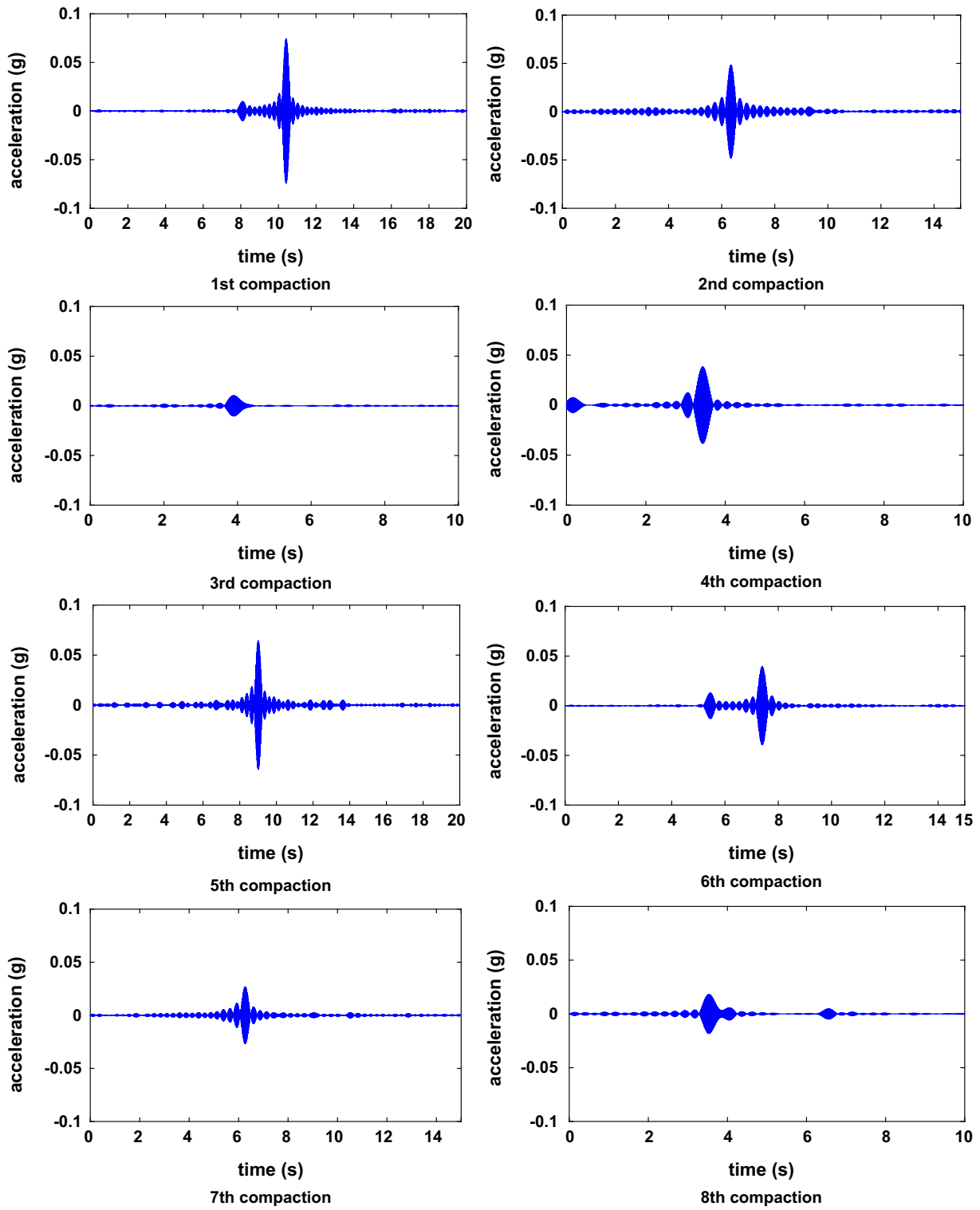


Fig. A3. measured acceleration of pavement in x-direction during vibration rolling.

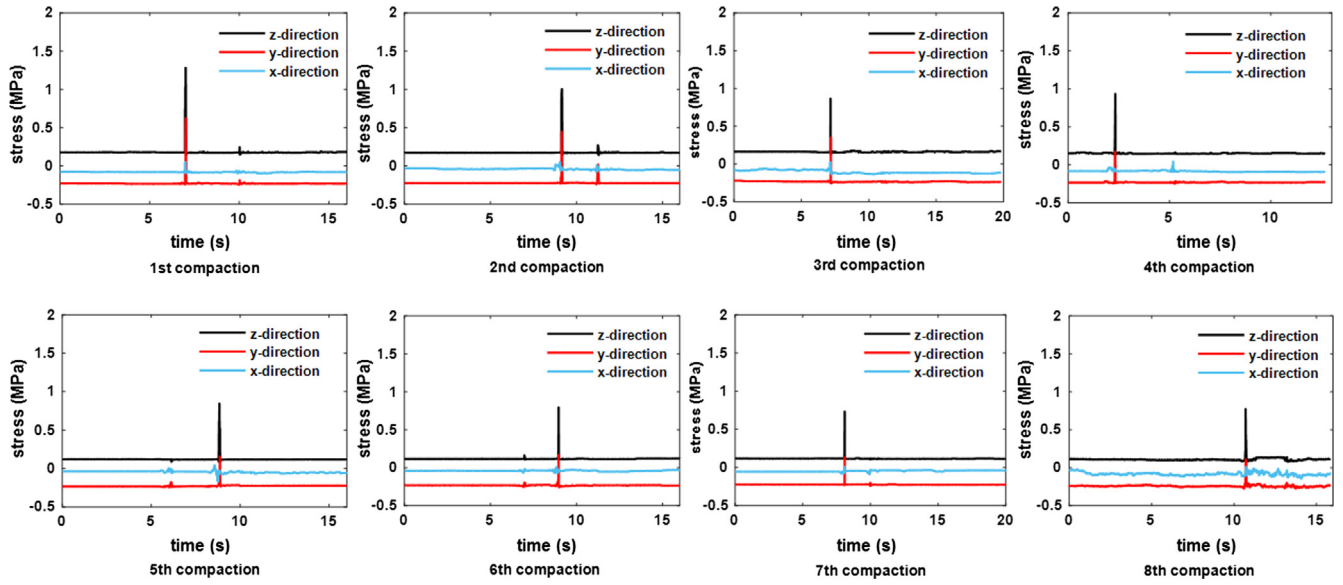


Fig. A4. Measured stress of pavement during vibration rolling.

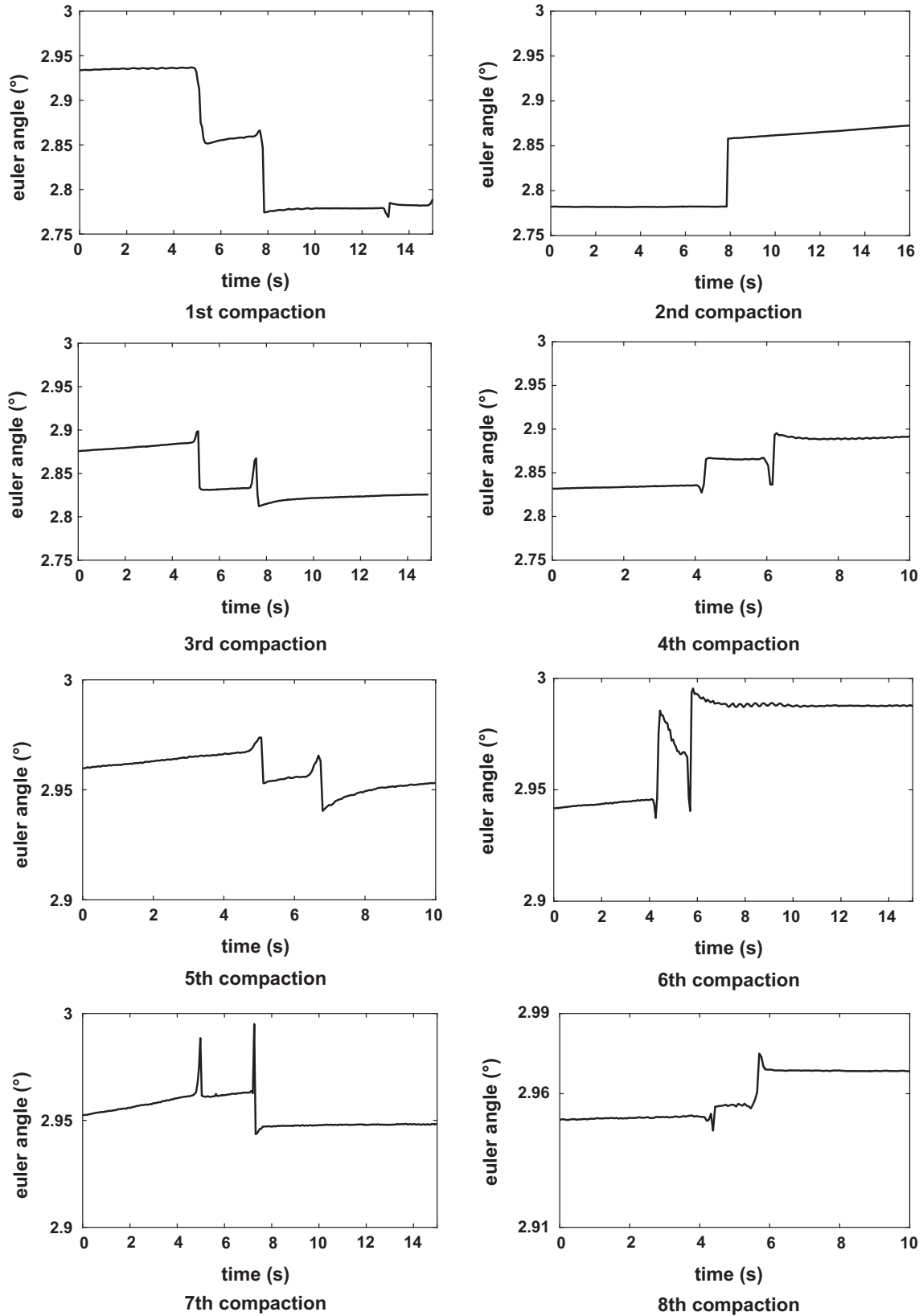


Fig. A5. Euler angle of SmartRock sensor around x-axis during vibration rolling.

## References

- [1] J. Yan, C. Zhang, M.H. Ding, Y. Tsai, An evaluation of highway work zone impact factors on driving safety using complicated indexes based on traffic simulation system, *Adv. Mater. Res.* 723 (2013) 943–950.
- [2] A.P. Peng, H.C. Dan, D. Yang, Experiment and numerical simulation of the dynamic response of bridges under vibratory compaction of bridge deck asphalt pavement, *Math. Prob. Eng.* 2019 (2019) 7020298, <https://doi.org/10.1155/2019/2962154>.
- [3] Y.C. Li, S. Li, R. Lv, P. Zhang, Y.Z. Xu, G.J. Hou, C. Cui, Research on failure mode and mechanism of different types of waterproof adhesive materials for bridge deck, *Int. J. Pavement Eng.* 16 (7) (2015) 602–608.
- [4] H.C. Dan, Z. Zhang, X. Liu, J.Q. Chen, Transient unsaturated flow in the drainage layer of a highway: solution and drainage performance, *Road Mater. Pavement Des.* 20 (3) (2019) 528–553.
- [5] R. Mallick, M. Radzicki, J. Daniel, J. Jacobs, Use of system dynamics to understand long-term impact of climate change on pavement performance and maintenance cost, *Transp. Res. Rec.* 2455 (2014) 1–9.
- [6] A.T. Pauli, M.J. Farrar, P.M. Harnsberger, Material property testing of asphalt binders related to thermal cracking in a comparative site pavement performance study, *Rilem Bookseries* 4 (3) (2012) 233–243.
- [7] H.C. Dan, L.H. He, L.H. Zhao, Experimental investigation on the resilient response of unbound graded aggregate materials by using large-scale dynamic triaxial tests, *Road Materials and Pavement Design.* 21(2) (2020) 434–421. <https://doi.org/10.1080/14680629.2018.1500300>.
- [8] W.S. Wang, Y.C. Cheng, P.L. Zhou, G.J. Tan, H.T. Wang, H.B. Liu, Performance evaluation of styrene-butadiene-styrene-modified stone mastic asphalt with basalt fiber using different compaction methods, *Polymers* 11 (6) (2019) 1006, <https://doi.org/10.3390/polym11061006>.
- [9] M. Mazari, Studying the Parameters Involved with Modulus-Based Construction Quality Control for Compaction of Unbound Pavement Layers, the University of Texas at EL PasoMI, USA, 2014.
- [10] H.C. Dan, Z. Zhang, J.Q. Chen, H. Wang, Numerical simulation of an indirect tensile test for asphalt mixtures using discrete element method software, *J. Mater. Civ. Eng.* 30 (5) (2018) 04018067.
- [11] H.C. Dan, J.W. Tan, J.Q. Chen, Temperature distribution of asphalt bridge deck pavement with groundwater circulation temperature control system under high- and low temperature conditions, *Road Mater. Pavement Des.* 20 (3) (2019) 528–553.
- [12] H.C. Dan, J.W. Tan, Y.F. Du, J.M. Cai, Simulation and optimization of road deicing salt usage based on Water-Ice-Salt Model, *Cold Reg. Sci. Technol.* 169 (2020) 102917.
- [13] Y.Q. Tan, H.P. Wang, S.J. Mao, H.N. Xu, Quality control of asphalt pavement compaction using fibre Bragg grating sensing technology, *Constr. Build. Mater.* 54 (2014) 53–59.
- [14] R.D. Horan, G.K. Chang, Q.W. Xu, V.L. Gallivan, Improving quality control of hot-mix asphalt paving with intelligent compaction technology, *Transp. Res. Rec.* 2268 (2012) 82–91.
- [15] P. Li, Z. Wang, Z. Ding, J. Zheng, The analysis of pavement quality indicator used in asphalt surface detection, *J. Comput. Theor. Nanosci.* 6 (1) (2012) 878–881.
- [16] P.C. Shangguan, I. Al-Qadi, A. Coenen, S. Zhao, Algorithm development for the application of ground-penetrating radar on asphalt pavement compaction monitoring, *Int. J. Pavement Eng.* 17 (3) (2014) 1–12.
- [17] L.S. Gao, H.C. Dan, L. Li, Response analysis of asphalt pavement under dynamic loadings: loading equivalence, *Math. Prob. Eng.* 2019 (2019) 7020298, <https://doi.org/10.1155/2019/7020298>.
- [18] V.D.B. Wim, V. Cedric, K. Patricia, C. Karolien, B. Johan, V.B. Philippe, The use of a non-nuclear density gauge for monitoring the compaction process of asphalt pavement, *IOP Conf. Ser.: Mater. Sci. Eng.* 236 (1) (2017) 012014.
- [19] Q. Xu, G.K. Chang, Experimental and numerical study of asphalt material geospatial heterogeneity with intelligent compaction technology on roads, *Constr. Build. Mater.* 72 (2014) 189–198.
- [20] H.C. Dan, Z.M. Zhou, J.Q. Chen, A.P. Peng, Experiment and numerical simulation of the dynamic response of bridges under vibratory compaction of bridge deck asphalt pavement, *Eng. Comput.* 36 (5) (2019) 1716–1743.
- [21] B.T. Huang, The DEM Numerical Simulation about Road Materials' Fabric and Mechanical Properties Evolution under Vibration Compaction, Southeast University, Nanjing, Jiangsu, China, 2009.
- [22] J.S. Chen, B.S. Huang, X. Shu, C.C. Hu, DEM simulation of laboratory compaction of asphalt mixtures using an open source code, *J. Mater. Civ. Eng.* 27 (3) (2015) 04014130.
- [23] F.Y. Gong, Y. Liu, X.D. Zhou, Z.P. You, Lab assessment and discrete element modeling of asphalt mixture during compaction with elongated and flat coarse aggregates, *Constr. Build. Mater.* 182 (2018) 573–579.
- [24] G.K. Chang, K. Mohanraj, W.A. Stone, D.J. Oesch, V. Gallivan, Leveraging intelligent compaction and thermal profiling technologies to improve asphalt pavement construction quality: a case study, *Transp. Res. Rec.* 2672 (26) (2018) 48–56.
- [25] X.Y. Zhu, S.J. Bai, G.P. Xue, J. Yang, Y.S. Cai, W. Hu, X.Y. Jia, B.S. Huang, Assessment of compaction quality of multi-layer pavement structure based on intelligent compaction technology, *Constr. Build. Mater.* 161 (2018) 316–329.
- [26] M. Wang, B. Gao, F. Shang, T. Wang, Application research of quality control technology of asphalt pavement based on GPS intelligent, *IOP Conf. Ser.: Mater. Sci. Eng.* 250 (1) (2017), <https://doi.org/10.1088/1757-899X/250/1/012029>.
- [27] W. Hu, B.S. Huang, X. Shu, M. Woods, Utilising intelligent compaction meter values to evaluate construction quality of asphalt pavement layers, *Road Materials and Pavement Design.* 18 (4) (2016) 1–12.
- [28] W. Hu, X.Y. Jia, X.Y. Zhu, H.R. Gong, G.P. Xue, B.S. Huang, Investigating key factors of intelligent compaction for asphalt paving: A comparative case study, *Constr. Build. Mater.* 229 (30) (2019) 116876.
- [29] A.G. Correia, H. Brandl, *Geotechnics for Roads, Rail Tracks and Earth Structures*, Crc Press, 2001.
- [30] D.L. Petersen, Continuous Compaction Control MnROAD Demonstration. Final Report, MN/RC-2005-07, Transportation research record, Washington DC, USA, 2005. <http://www.lrrb.org/pdf/200507.pdf>.
- [31] R.V. Rinehart, M.A. Mooney, Instrumentation of a roller compactor to monitor vibration behavior during earthwork compaction, *Autom. Constr.* 17 (2) (2008) 144–150.
- [32] M.A. Mooney, P.B. Gorman, J.N. Gonzalez, Vibration-based health monitoring of earth structure, *Struct. Health Monit.* 4 (2) (2005) 137–152, <https://doi.org/10.1177/1475921705049759>.
- [33] S.S. Liu, H. Huang, T. Qiu, L. Gao, Comparison of laboratory testing using SmartRock and discrete element modeling of ballast particle movement, *J. Mater. Civ. Eng.* 29 (3) (2017) D6016001.
- [34] S.S. Liu, T. Qiu, Y. Qian, H. Huang, E. Tutumluer, S.H. Shen, Simulations of large-scale triaxial shear tests on ballast aggregates using sensing mechanism and real-time (SMART) computing, *Comput. Geotech.* 110 (2019) 184–198.
- [35] S.S. Liu, H. Huang, T. Qiu, J. Kown, Effect of geogrid on railroad ballast particle movement, *Transp. Geotech.* 9 (2016) 110–112.
- [36] H. Huang, S.S. Liu, T. Qiu, Identification of railroad ballast fouling through particle movements, *J. Geotech. Geoenviron. Eng.* 144 (4) (2018) 02818001.
- [37] X. Wang, S.H. Shen, H. Huang, Z.D. Zhang, Towards smart compaction: particle movement characteristics from laboratory to the field, *Constr. Build. Mater.* 218 (2019) 323–332.
- [38] Ministry of Transport of the People's Republic of China. Standard test methods of bituminous mixtures for highway engineering, JTG E20, China Communications Press, Beijing, China, 2019.
- [39] L. Chen, H.P. Zheng, A comparative study of the time and frequency domains in dynamic analysis of vibratory roller, *J. Shijiazhuang Univ. Appl. Technol.* 26 (6) (2014) 36–39.
- [40] B.A. Chadbourne, D. Newcomb, V. Voller, et al., *An Asphalt Paving Tool for Adverse Conditions*, 1998.
- [41] G.X. Song, X.G. Chen, Y.F. Yu, Research on numerical simulation about dynamic response of silty clay subgrade under impact and grind, *J. Build. Sci. Eng.* 33 (02) (2016) 24–30.
- [42] J. Zhang, L.Y. Wei, S.B. Ma, T. Wang, Field test and numerical simulation of dynamic response of semi-rigid base asphalt pavement under moving vehicle load, *J. Highway Transp. Res. Dev.* 33 (10) (2016) 19–24.
- [43] B. Li, S.J. Jiao, *Vibratory Roller and Vibratory Compaction*, China Communications Press, China, 2001.
- [44] X.L. Zhi, X.X. Jiang, A.M. Sha, Pavement subbase course stress by vibrating compaction on course, *J. Xi'an Highway Univ. (Natural Science Edition)*, 23 (3) (2003) 33–36.
- [45] M.X. Li, Simulation Analysis of Relationship between Road Stiffness and Vibration Acceleration, Chongqing Jiaotong University, Chongqing, China, 2016.
- [46] R.L. Peterson, K.C. Mahboub, R.M. Anderson, E. Masad, L. Tashman, Comparing superpave gyratory compactor data to field cores, *J. Mater. Civ. Eng.* 16 (1) (2004) 78–83.